Scientia Iranica A (2021) 28(5), 2596–2612

Sharif University of Technology
Scientia Iranica
Transactions A: Civil Engineering
http://scientiairanica.sharif.edu

An integrated method for sustainable performance-based optimal seismic design of RC frames with non-prismatic beams

A. Kaveh[a,*], L. Mottaghi[b], and R.A. Izadifard[b]

a. *School of Civil Engineering, Iran University of Science and Technology, Tehran, Iran.*
b. *Department of Civil Engineering, Imam Khomeini International University, Qazvin, Iran.*

Received 30 May 2021; received in revised form 6 June 2021; accepted 5 July 2021

KEYWORDS
Performance-based seismic design;
Optimal cost;
Optimal CO_2 emissions;
Prismatic beams;
Non-prismatic beams;
Metaheuristic algorithms.

Abstract. In the performance-based optimal seismic design, one attempts to obtain structural design variables to meet the minimum objective function satisfying the strength-based and performance-based constraints. A limited number of studies have been conducted on the performance-based optimal seismic design of Reinforced Concrete (RC) frames. On the other hand, due to the significance of environmental impacts, further study on the design of RC buildings aiming at reducing CO_2 emissions is required. In this study, a computational procedure is developed for performance-based optimal seismic design of RC frames with prismatic beams and frames with non-prismatic beams. The objective functions consist of minimizing the cost and CO_2 emissions. Nonlinear pushover analysis was performed to analyze the frames. The described procedure was then applied to a four-story RC frame, and the relationship between optimal cost and optimal CO_2 emissions was investigated in the case of frames with prismatic beams and those with non-prismatic beams.

1. Introduction

Performance-Based Seismic Design (PBSD) is a methodology for designing structures and has been frequently considered by earthquake engineers. It also has been introduced by various guidelines to rehabilitate existing buildings as well as designing new ones. The purpose of PBSD is to increase the safety of the structure against natural hazards and to design a structure with predictable performance. Based on the importance of the structure and its performance after an earthquake, the codes classify possible damages and determine the level of performance. In accordance with FEMA-273 [1], Immediate Occupancy (IO), Life Safety (LS), and Collapse Prevention (CP) are considered as performance levels. Pushover analysis is a very popular technique for nonlinear analysis of structures and seismic demand assessment of structures in PBSD.

In traditional methods (trial and error) for designing the structures, the required analysis is repeated until achieving a reasonable design and the quality of the design produced by traditional methods depends on the engineer's experience and ability. The final design obtained by this method is not sufficient to meet both economic and safety criteria simultaneously. Given this, studies have been carried out using optimization methods to solve problems. In these methods, the objective functions, constraints, type of structural analysis, and optimization process may be different. In a number of studies on the performance-based

*. *Corresponding author. Tel.: +98 21 44429493; Fax: +98 21 77240398*
E-mail address: alikaveh@iust.ac.ir (A. Kaveh)

doi: 10.24200/sci.2021.58452.5728

optimal seismic design, the objective function was to minimize the construction cost [2–7]. However, the main objective of some other studies was to minimize the total life cycle costs [8–11]. The total life cycle costs come from the initial operation cost as well as other costs of maintenance, damage, and repair, which are expressed as functions of their seismic performance level in the probability of failure. Park et al. [12] used a process for multi-objective performance-based optimal seismic design in Reinforced Concrete (RC) buildings with prismatic beams. In their study, the objective functions involve the cost of materials, CO_2 emission, and seismic performance.

Nowadays, reduction of greenhouse gas emissions is a major global challenge. To be specific, CO_2 emissions account for the largest amount of greenhouse gases, i.e., about 77% of greenhouse gases since 2004 [13]. The environmental impact of construction industry on greenhouse gas emissions is considerable. Therefore, strategies have been employed to reduce these effects. One strategy is use of optimization techniques during the structural design, where the objective function reduces the amount of carbon dioxide emissions. Reinforced concrete buildings are made of two types of material, i.e., concrete and steel, and they have different amounts of carbon dioxide emissions. Therefore, they have high potential to reduce CO_2 emissions in optimization methods. Camp et al. [14] optimally designed RC frames using big bang-big crunch optimization algorithm. In their study, the objective functions were the minimization of the CO_2 emissions and costs. In another study, Camp and Assadollahi [15] minimized the cost and CO_2 emissions of RC footings. Yepes et al. [16] proposed a methodology for the optimal design of RC cantilever retaining walls using a hybrid multi-start optimization strategic method based on Variable Neighborhood Search Threshold Acceptance Strategy (VNS-MTAR) algorithm to minimize the cost and CO_2 emissions. Kaveh et al. [17] investigated the relationship between the optimal cost and optimal carbon dioxide emissions in the design of RC frames with different heights. The optimal solutions for each frame were obtained through three metaheuristic algorithms. Mergos [18] evaluated the effects of factors such as ductility classes, Peak Ground Accelerations (PGAs), and concrete classes on the reduction of CO_2 emissions in design of seismic-resistant RC frames. Yeo and Potra [19] developed a methodology to optimally design RC frames with the objectives of minimizing CO_2 emission and economic cost. They investigated a portal RC frame under gravitational and lateral loads. They also stated that depending on the parameters considered in calculations, the design aiming to minimize CO_2 emission would reduce it by 5–10% compared to that of the optimal design aiming to minimize cost. Oh et al. [20] established a relationship among optimal carbon dioxide emissions, optimal cost, and structural parameters of composite columns (concrete-filled steel tube), in which the type of section (circular and rectangular), number of materials, and strength of each material were regarded as design variables.

Furthermore, a number of studies have been conducted to optimally design frames characterized by non-prismatic elements. In non-prismatic beams, the values of width, depth or both of them may vary. An acceptable height for the floors of buildings can be determined using these types of beams. They are mostly used in bridges, industrial structures, amphitheaters, sport arenas, parking, etc. McKinstray et al. [21] optimally designed single-span industrial steel frames with three types of sections, namely rolled, fabricated, and non-prismatic. Kaveh et al. [22] optimally designed three dimensional steel structures with non-prismatic beams and columns. The optimal weights of frames with non-prismatic elements were compared with the optimal design of frames with prismatic elements. Yavari et al. [23] optimized CO_2 emissions and cost of concrete slab frame bridges during the design phase, with the slab being considered as non-prismatic. Kaveh et al. [24] presented a methodology for the sustainable design of RC frames with non-prismatic beams and investigated the relationship between the optimal cost and optimal carbon dioxide emissions while designing these frames.

A review of the literature shows that a limited number of studies have been conducted on the Performance Based Optimal Seismic Design (PBOSD) of reinforced concrete buildings with the objective of minimizing carbon dioxide emissions. In addition, few studies have been conducted to optimally design RC frames using non-prismatic elements. In a previous study, the authors investigated the relationship between the optimal cost and optimal CO_2 emission in the case of RC frames with non-prismatic beams [24]. They employed equivalent linear static analysis to determine the demand for elements and control the strength-based constraints for structures, where the nonlinear behavior of the structures and performance-based constraints were not taken into account.

In this study, RC frames with prismatic beams and RC frames with non-prismatic beams were optimized with the objective of minimizing CO_2 emission and construction cost. The nonlinear static (pushover) analysis was carried out using the structural optimization strategy to optimally design frames at the performance levels. The relationship between the optimal cost and optimal CO_2 emissions of frames at performance levels was also investigated. Five metaheuristic algorithms consisting of the Particle Swarm Optimization (PSO), Colliding Bodies Optimization (CBO), Enhanced Colliding Bodies Opti-

mization (ECBO), Vibrating Particles System (VPS), and Enhanced Vibrating Particles System (EVPS) were used in the optimal design of the frames with prismatic beams at the IO performance level. The most competent algorithm was then selected and used to solve the remaining problems.

2. Formulation of optimal design

2.1. Performance-based optimal seismic design

In the performance-based optimal design, the problem formulation can be obtained based on Eq. (1). Here, $f(x)$ is the objective function, g_j^{SBD} the strength-based constrains, g_j^{PBD} the performance-based constraints, and x the design variables. First, equivalent static analysis was carried out for structures, and strength-based constraints based on ACI 318-08 [25] code were checked. Then, the performance-based constraints that were related to the maximum inter-story drift were checked under nonlinear static analysis at three performance levels based on FEMA code [1]:

$$\begin{aligned} &\min\ f(x)\\ &g_j^{SBD}, \qquad j=1,...,m\\ &g_j^{PBD}, \qquad j=1,...,k\\ &x^L \le x \le x^U. \end{aligned} \tag{1}$$

According to the ACI 318-08 code, the following load combinations (Eq. (2)) were used in the equivalent static analysis. Here, D is the dead load, L the live load, and E the lateral equivalent static loads:

$$Q_G^{SBD}:\ \begin{aligned} &1.2D+1.6L,\\ &1.2D+L\pm 1.4E,\\ &0.9D\pm 1.4E. \end{aligned} \tag{2}$$

In pushover analysis, the lateral load should be incrementally applied to the building while the gravity load is constantly applied. In this study, the load combination (Eq. (3)) and lateral load with the pattern based on the first mode shape are used in pushover analysis:

$$Q_G^{PBD}=1.1(D+L). \tag{3}$$

In nonlinear static analysis, it is assumed that the structure response is associated with an equivalent single degree of freedom system. The model of structures is pushed by the lateral load until the displacement of the roof reaches the target displacement or mathematical instability occurs. Based on FEMA-356 [26], the target displacement is calculated as follows:

$$\delta t = C_0 C_1 C_2 C_3 S_a \frac{T^2}{4\pi^2} g, \tag{4}$$

where C_0 is the modification factor for relating the spectral displacement of a single degree of freedom to the roof of multi degrees of freedom. In addition, C_1 is the modification factor for converting the calculated displacements from the linear elastic response to the expected maximum inelastic displacements; C_2 is the modification factor which represents the effect of hysteresis shape on the maximum displacement response. The value of this coefficient is determined based on the structural performance level, type of frame, and period of the structure. Moreover, C_3 is the modification factor representing the increase in displacement due to the dynamic effects of P-Delta. Finally, S_a is the spectral response acceleration versus structural period domain calculated at three performance levels, as shown in the following:

$$\begin{aligned} &\left(\frac{S_{XS}^i}{B_S}\right)\left(0.4+3\frac{T}{T_0}\right) \quad \text{for} \quad 0<T<0.2T_0^i,\\ &S_a^i=\frac{S_{XS}^i}{B_S} \qquad\qquad \text{for} \quad 0.2T_0^i<T<T_0^i\\ &i=IO,LS,CP,\\ &\frac{S_{X1}^i}{B_1 T} \qquad\qquad \text{for} \quad T>T_0^i, \end{aligned} \tag{5}$$

where T is the elastic fundamental period of the structure obtained from the modal analysis of the structure and i represents three performance levels of IO, LS, and CP.

T_0 is given by Eq. (6), and B_S and B_1 in accordance FEMA-273 are assumed to be equal to 1.

$$T_0^i=(S_{X1}^i/B_S)/(S_{XS}^i/B_1), \tag{6}$$

$$S_{X1}^i=F_v^i S_1^i, \tag{7}$$

$$S_{XS}^i=F_a^i S_S^i, \tag{8}$$

where F_a^i and F_v^i are the site coefficients that are determined based on the site class and the values for response acceleration parameters S_S^i and S_1^i. Table 1 [27] lists the parameters for site class D.

The procedure for automatic performance-based optimal seismic design through the selected algorithms is presented in Figure 1.

2.2. Design variables and database for sections

In this study, 11 variables for beams and 4 variables for columns were taken into account. Figure 2 shows the variables for non-prismatic beams. These variables include the dimensions of the cross-sections of column elements (depth and width), diameter and number of

Table 1. Performance-level site parameters for site class of D.

Performance level	Earthquake level	S_S (g)	S_1 (g)	F_a	F_v	T_0 (s)
IO	20%/50	1.143	0.403	1.04	1.60	0.542
LS	10%/50	1.587	0.560	1.00	1.50	0.529
CP	2%/50	2.380	0.840	1.00	1.50	0.529

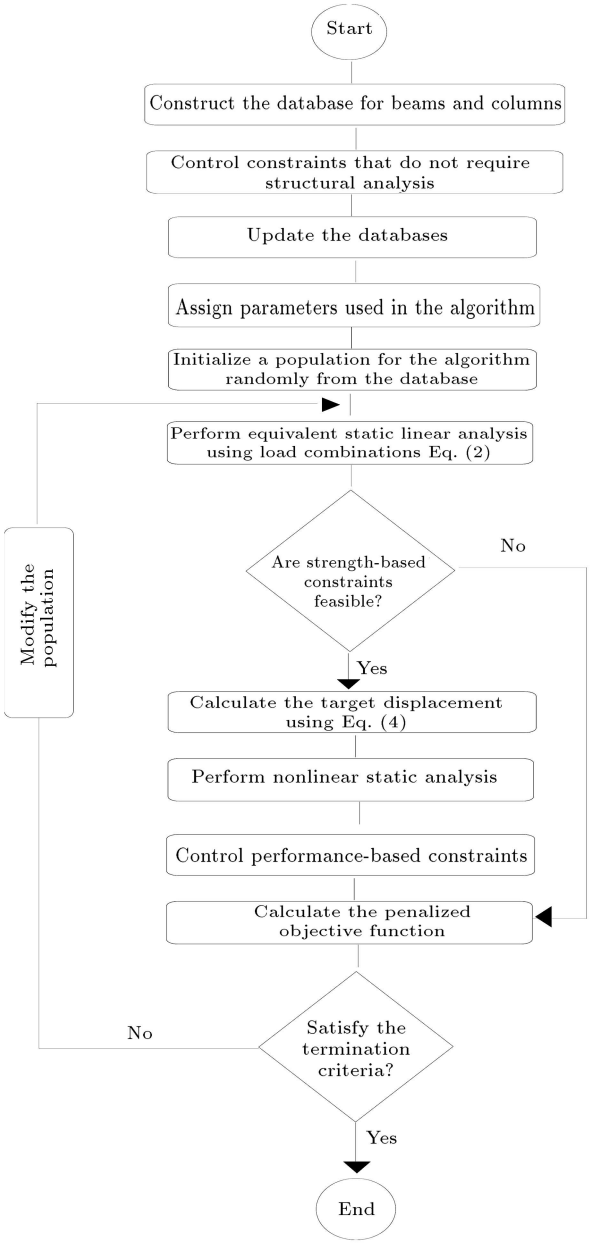

Figure 1. Flowchart of the optimization by the selected algorithms.

longitudinal bars of the columns, depth of the cross-section of beams in prismatic zone (h_2), depth of the cross-section of beams in non-prismatic zone (h_1), diameter and number of longitudinal bars in prismatic section of beams (As_2) (at the top and bottom of

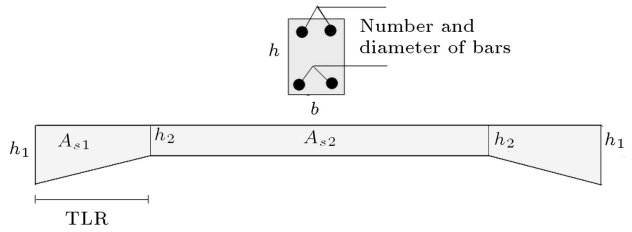

Figure 2. Variables and shape of a non-prismatic beam.

sections), diameter and number of longitudinal bars in the non-prismatic section of beams (As_1) (at the top and bottom of sections), and length of tapered section that is defined as the percentage of the length of the beam (Tapered Length Ratio (TLR)). The width of cross-section for beams is assumed to be constant. The search space parameters for beams and columns are shown in Table 2.

In order to formulate the variables in the discrete form and reduce the constraint to solve the problem, two databases were created for beams and columns. In these databases, those constraints that do not require structural analysis, such as the percentage of permissible bars, depth-to-width ratio, etc., can be controlled based on the ACI 318-08 code and removed from the database.

Database for beam sections

In the formulation of database for beams, the width, depth, cross-section area, moment of inertia, number and diameter of bars, bending capacity, and cost or amount of CO_2 emission per unit length of the beams are given. In the cross-sections of beams, the depth-to-width ratio varies between 1 and 3.

The moment-resisting capacity of a beam section is defined by Eq. (9):

$$M_n = A_s f_y \left(d - \frac{a}{2}\right), \tag{9}$$

where A_s is the total area of tensile reinforcing bars, f_y the yield strength of bars, d the distance of the compressive edge of the section to the center of the tensile bars, and a the depth of the equivalent rectangular stress block which is defined as follows:

$$a = \frac{A_s f_y}{0.85 f'_c b}, \tag{10}$$

Table 2. Search space parameters.

		Width (mm)	Depth (mm)	Number of bars	Bar size	TLR %
Column	Min	250	250	4	3	
	Max	1200	1200	12	11	
	Increment	50	50	2	1	
Beam	Min	350	350	2	3	10
	Max	350	1050	5	11	25
	Increment		50	1	1	5

where f'_c is the compressive strength of the concrete and b the width of the cross-sections.

Database for column sections

In the formulation of database for column sections, width, depth, area of cross-section, moment of inertia, number and diameter of bars, cost or the amount of CO_2 emission per unit length of the column are also given. Furthermore, as shown in Figure 3, the parameters related to the $P-M$ interaction diagram are measured based on the ACI code and then, they are saved in the database. In the cross-section of the columns, the rebars are distributed along all four faces of sections according to the patterns, as shown in Figure 4.

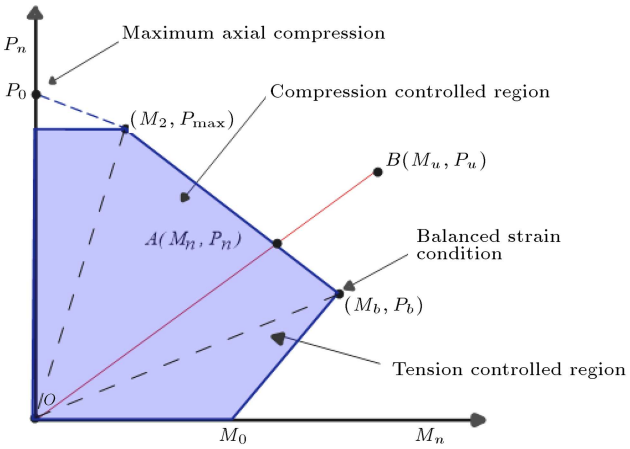

Figure 3. Column load-moment interaction diagram.

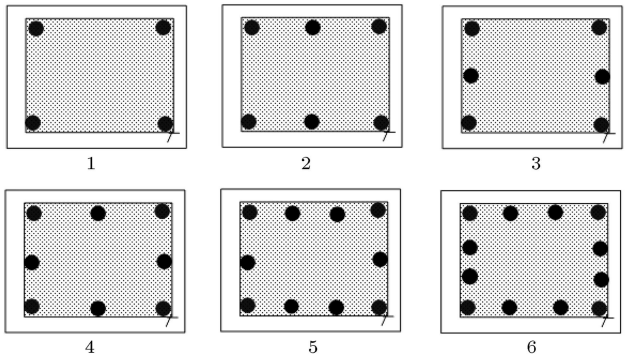

Figure 4. Column reinforcement patterns.

2.3. Objective functions

In this study, the objective of optimization was to minimize the construction cost and amount of CO_2 emissions, as expressed by Eq. (11). Here, n_b and n_c are the number of beams and columns, respectively; b_i, h_i, A_{si}, and L_i are the width, depth of the sections, area of the bars, and length of the beams and columns, respectively; t_i is the thickness of the slab that is considered to be 290 mm. In addition, C_C, C_s, C_f, and C_t are the unit rate of concrete, bars, formwork, and scaffolding, respectively, and their values are listed in Table 3. The parameter γ_s is the unit weight of steel calculated as 7849 kg/m^3. In the objective function of CO_2 emission, scaffolding is neglected.

$$f_K = \sum_{i=1}^{n_b+n_c} \{C_C b_i h_i + C_s \gamma_s A_{si}\} L_i + \sum_{i=1}^{n_b} \{C_f (b_i + 2(h_i - t_i)) + C_t b_i\} L_i + \sum_{i=1}^{n_c} \{2C_f (b_i + h_i)\} L_i. \quad (11)$$

2.4. Design constraints

According to design codes, strength-based and performance-based constraints should be checked during the design process. Equivalent static analysis was done for structures, and the strength-based constraints were checked based on ACI code; then, the performance-based constraints related to the maximum inter-story drift were controlled through pushover analysis at three performance levels. The variables that do not satisfy these constraints are removed from calculations. One method used for avoiding repetitions of calculations for these variables is the penalty function method. In this method, through incorporation of a penalty value to the objective function based on the extent of violation of the constraints, the problem turns into an unconstrained problem. In Eq. (12), the parameters, g_i, x, and n are the penalty of the ith constraint, vector of design variables, and number of constraints, respectively. Furthermore, f_p is the penalized objective function, and f is the value of the

Table 3. Unit prices and CO_2 emissions [14].

Description	Unit	Cost (€)		CO_2 (kg)	
		Beam	Column	Beam	Column
Steel B-500	kg	1.3	1.3	3.01	3.01
Concrete (40 MPa)	m^3	105.93	105.17	143.77	143.77
Form work	m^2	25.05	22.75	3.13	8.9
Scaffolding	m^2	38.89	–	–	–

objective function. In this study, the value of k is considered as 1.5.

$$f_p(x) = f \times \left(1 + \sum_{i=1}^{n} \max(0, g_i(x))\right)^k. \quad (12)$$

2.4.1. Strength-based constraints

Constraints of the beams

In order to evaluate the moment capacity of the RC beams, the penalty function is measured, as shown in Eq. (13). In non-prismatic beams, this constraint is examined in Sections 1–5 as in Figure 5. Section 3 is where the positive bending moment has the maximum value.

$$g_1 = \frac{|M_u| - \phi M_n}{\phi M_n}, \quad (13)$$

where M_u is the ultimate applied bending moment under the applied loading and ϕ is the strength reduction factor which is equal to 0.9. In addition, M_n is the moment capacity of the RC beams, as defined in Eq. (9).

According of ACI code, the ratios of minimum and maximum reinforcement of the beam sections are limited. The penalties of these constraints are as follows:

$$\rho_{\min} = \frac{\sqrt{f'_c}}{4f_y} \geq \frac{1.4}{f_y}, \qquad g_2 = \rho_{\min} - \rho, \quad (14)$$

$$\rho_{\max} = 0.85\beta_1 \frac{f'_c}{f_y} \frac{600}{600 + f_y}, \qquad g_3 = \rho - \rho_{\max}. \quad (15)$$

In order to control the deflection of the beams, the following penalty was employed in this study.

$$h_{\min} = \frac{L}{21}, \qquad g_4 = \frac{h_{\min} - h}{h_{\min}}. \quad (16)$$

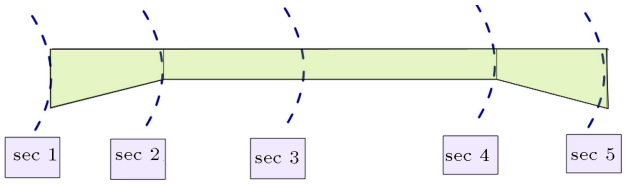

Figure 5. Critical sections along the non-prismatic beams.

In the section of beams, in case the effective depth (d) is lower than the compression-block depth (a), the penalty is defined as follows:

$$g_5 = \frac{a - d}{d}. \quad (17)$$

The minimum distance between the bars should be limited. The penalty of this constraint is defined as:

$$g_6 = \frac{s_{\min} - s}{s_{\min}}, \qquad s_{\min} = \max(d_b, 1 \text{ inch}). \quad (18)$$

According to Figure 2, secondary height (h_2) must not be greater than the initial height (h_1); therefore, the penalty can be defined as:

$$g_7 = \frac{h_2 - h_1}{h_2}. \quad (19)$$

Constraint of columns

In case the combination of (M_u, P_u) under the applied loads falls inside the interaction $P - M$ diagram, a column section is suitable. The penalty function for the capacity of the columns can be expressed as follows:

$$g_8 = \frac{L}{L_0} - 1. \quad (20)$$

In Figure 3, l is the distance between the origin of the interaction diagram (O) and Point (B) indicating the position of combination (M_u, P_u), and l_0 is the radial distance between the origin of the interaction diagram (O) and Point (A) indicating the intersection point of the vector l with the interaction diagram.

The total area of bars (A_s) in the cross-section of the RC column is limited between 1% and 8% of the cross section (A_g). The penalties of the minimum and maximum reinforcement for the columns are expressed as:

$$g_9 = \frac{0.01 \times A_g}{A_S} - 1 \leq 0, \quad (21)$$

$$g_{10} = \frac{A_S}{0.08 \times A_g} - 1 \leq 0. \quad (22)$$

The function penalty defined for the distance between longitudinal bars is:

$$g_{11} = \frac{s_{\min} - s}{s_{\min}}, \qquad s_{\min} = \max(1.5d_b, 1.5 \text{ inch}). \quad (23)$$

The dimensions of columns in each story should be smaller than or equal to those of columns on the bottom story; hence, the constraints can be expressed as follows:

$$g_{12} = \frac{b_T}{b_B} - 1, \tag{24}$$

$$g_{13} = \frac{h_T}{h_B} - 1, \tag{25}$$

where B and T present the bottom column and top column, respectively; and b and h are the width and depth of the column cross-section, respectively.

2.4.2. Performance based constraint

Lateral drift is an important indicator for measuring damage in structures that should be controlled in seismic design [28]. Performance-based constraints are expressed as lateral drift at different performance levels, as shown in the following:

$$g_{14} = \frac{\theta^{IO}_{\max}}{\theta^{IO}_{allow}} - 1, \tag{26}$$

$$g_{15} = \frac{\theta^{LS}_{\max}}{\theta^{LS}_{allow}} - 1, \tag{27}$$

$$g_{16} = \frac{\theta^{CP}_{\max}}{\theta^{CP}_{allow}} - 1, \tag{28}$$

where $\theta^{IO}_{\max}$, $\theta^{LS}_{\max}$, and $\theta^{CP}_{\max}$ are the maximum inter-story drift of frame at the performance levels of IO, LS, and CP, respectively. Further, based on FEMA-273, θ^{IO}_{allow}, θ^{LS}_{allow}, and θ^{CP}_{allow} are allowable drifts that are determined to be 1%, 2%, and 4% for IO, LS, and CP performance levels, respectively.

2.5. Structural analysis model

The finite element software Opensees [29] was employed in this study to model the frames. Linear static and nonlinear static analyses of the structures and determination of the demand of the elements are performed using the mentioned software package. The limitations of the ACI and FEMA codes and optimization algorithm were handled in MATLAB software [30]. While the beams and columns were modeled with the *elastic beam column element* in the linear static analysis, *nonlinear beam column element* with distributed plasticity was used to model beams and columns in nonlinear static analysis. Moreover, to model non-prismatic beams upon dividing each non-prismatic element into 12 parts, the step-by-step method was employed. Nonlinear concrete and steel material properties are provided in Table 4. According to this table, the effects of confined and unconfined parts of the fiber section are imposed on the definition of concrete properties. Further, the P-Delta effects were included as geometric transformation. Hence, both material and geometry nonlinearity were taken into account.

3. Optimization algorithms

In this section, the algorithms used in this paper are introduced. PSO is a well-known algorithm that has been widely employed in many studies. In addition, ECBO, EVPS, VPS, and CBO algorithms have been recently developed and compared with the previously developed ones, and they were found to be comparatively efficient.

3.1. Colliding Bodies Optimization (CBO)

The CBO algorithm [31] is inspired by the laws of momentum and energy of the physics, where the bodies collide with each other and move to the lower cost. Each of Colliding Bodies (CB) is a solution candidate that contains a number of variables. The procedure of the CBO algorithm can be expressed as:

Step 1: First, the initial position of each CB is randomly obtained in the search space as follows:

Table 4. The properties of materials.

Concrete (uniaxial material concrete01)				
Material type	f'_c **(MPa)**	ε_{c_0}	f'_{cu} **(MPa)**	ε_{cu}
Core concrete of beams (confined)	44	0.00296	15.3	0.0148
Core concrete of columns (confined)	48	0.0032	16.8	0.048
Cover concrete (unconfined)	40	0.0025	14	0.0055

Steel (uniaxial material steel01)			
Material type	f_y**(MPa)**	E_0	**Hardening ratio**
Reinforcing steel	500	2e5	0.01

$$x_i^0 = x_{\min} + rand(x_{\max} - x_{\min}), \quad i = 1, 2, ..., n, \quad (29)$$

where x_i^0 is the initial position of the ith CB; $x_{\max}$ and $x_{\min}$ are the minimum and maximum allowable values of variables, respectively. The rand parameter is a random value in the range [0, 1], and n is the number of CB.

Step 2: In the next step, the mass of each object is determined as follows:

$$m_k = \frac{\frac{1}{fit(k)}}{\sum_{i=1}^{n} \frac{1}{fit(i)}}, \qquad k = 1, 2, ..., n, \quad (30)$$

where $fit(i)$ presents the objective function value for the ith colliding body and n is the number of populations. Arranged in a descending order, the objects are divided into two equal groups of stationary and moving objects. To improve the position of moving objects and move the stationary objects toward a better position, the moving object moves toward a stationary object; hence, collision occurs (Figure 6).

Step 3: The velocity of stationary objects before collision is zero, and the velocity of the moving objects before collision is calculated as follows:

$$v_i = 0, \qquad y = 1, 2, ..., \frac{n}{2}, \quad (31)$$

$$v_i = x_{i-\frac{n}{2}} - x_i, \qquad i = \frac{n}{2} + 1, ..., n. \quad (32)$$

Step 4: After the collision of the moving and stationary objects, the velocity of the objects is calculated as follows:

Stationary objects:

$$v_i' = \frac{(m_{i+\frac{n}{2}} + \varepsilon m_{i+\frac{n}{2}}) v_{i+\frac{n}{2}}}{m_i + m_{i+\frac{n}{2}}}, \qquad i = 1, 2, ..., \frac{n}{2}. \quad (33)$$

Moving objects:

$$v_i' = \frac{(m_i - \varepsilon m_{i-\frac{n}{2}}) v_i}{m_i + m_{i-\frac{n}{2}}}, \qquad i = \frac{n}{2} + 1, ..., n. \quad (34)$$

Coefficient of restitution (ε) is defined as:

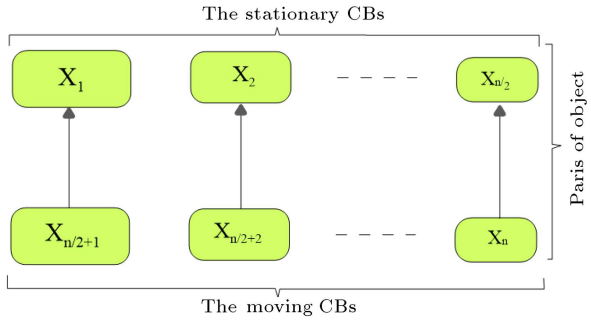

Figure 6. The pairs of objects for collision.

$$\varepsilon = 1 - \frac{iter}{iter_{\max}}. \quad (35)$$

Step 5: Through the generated velocities after the collision and their old position, the new positions of the objects for both groups are updated as follows:

The new position of moving object:

$$x_i^{new} = x_{i-\frac{n}{2}} + rand^o v_i', \quad i = \frac{n}{2} + 1, \frac{n}{2} + 2, ..., n, \quad (36)$$

where x_i^{new} is the new position of the ith CBs, $x_{i-\frac{n}{2}}$ is the old position of the ith stationary CB, and rand is a random vector uniformly distribution in the range of $(-1, 1)$; further, v_i' is the velocity of the ith moving CB after collision. The sign "^{o}" denotes element-by-element multiplication.

The new position of the stationary object can be obtained by:

$$x_i^{new} = x_{i-\frac{n}{2}} + rand^o v_i', \quad i = \frac{n}{2} + 1, \frac{n}{2} + 2, ..., n, \quad (37)$$

where x_i^{new} is the new position of the ith CBs, $x_{i-\frac{n}{2}}$ the old position of ith stationary CB and v_i' the velocity after the collision of the ith stationary CB.

Step 6: The procedure is repeated from Step 2 until a terminating criterion is accepted.

3.2. Enhanced Colliding Bodies Optimization (ECBO)

The performance of the CBO algorithm was modified using two techniques. These techniques were employed to obtain reliable solutions and fast convergence. This algorithm was developed by Kaveh and Ilchi Ghazaan [32] that have been used in many studies, see [33,34]. Colliding Memory (CM) was employed to modify the obtained solutions in each step. It stores some of the best CBs in the previous population in each iteration and replaces them with the worst CBs in the current population. Introducing new objects to the population can improve the performance of the algorithm without increasing the computational cost. To improve the exploration capabilities and prevent premature convergence, a component of CBs is randomly regenerated in each iteration. The value for this parameter, which is expressed as Pro, is in the range of (0, 1). The steps of this algorithm are as follows:

Step 1: The initial position of all CBs vectors with a number of variables is randomly selected;

Step 2: The mass of each CB is calculated based on Eq. (30);

Step 3: Some of the vectors of the best CBs are stored in CM and replaced by the worst ones;

Step 4: The objects are divided into two equal groups of stationary and moving objects based on Figure 6;

Step 5: The velocity of the moving objects before collision is obtained through Eq. (32);

Step 6: The velocity of objects after collision is obtained through Eqs. (33) and (34);

Step 7: The new position of objects is obtained using Eqs. (36) and (37);

Step 8: The Pro parameter is compared with the random number rni $(i = 1,2,...,n)$; If $Pro > rni$, a CB is randomly selected from both moving and stationary groups and one related component regenerate;

Step 9: Return to Step 2 until terminating criterion is satisfied.

3.3. Vibrating Particles System (VPS)

VPS algorithm was proposed by Kaveh and Ilchi Ghazaan [35]. It is inspired by the free vibration of single-degree-of-freedom systems with viscous damping. It is made up of particles that contain a number of variables. In this algorithm, three parameters with different weights are defined to form the new position: HB, the historically best position of the entire population; GB, a good particle; and BP, a bad particle. With a combination of the current population and historically best position, a balance between diversification and intensification is established and the particles approach equilibrium positions. The procedure of this algorithm is defined as:

Step 1: In this algorithm, the initial position of all particles in the research space is randomly determined.

$$x_i^j = x_{\min} + rand(x_{\max} - x_{\min}), \quad i = 1,2,...,n, \quad (38)$$

where x_i^j is the jth variable of the particle i; $x_{\min}$ and $x_{\max}$ are the minimum and maximum allowable values of the research space. Further, $rand$ is a rand number between [0,1], and n represents the number of particles;

Step 2: The value of the target function is calculated for each particle;

Step 3: For each particle, three balanced positions with different weights are defined, and their positions are updated. The positions are HB (the historically best position of the entire population), GP (a good particle), and BP (a bad particle). In order to select good and bad particles, the population must be arranged in an ascending order according to the values of their objective function. Finally, the GP and BP particles are randomly selected from the first and second halves, respectively. The positions are updated by:

$$x_i^j = w_1.[D.A.rand1 + HB^j] + w_2.[D.A.rand2 + GP^j] + w_3.[D.A.rand3 + BP^j], \quad (39)$$

where w_1, w_2, w_3 are three parameters used for measuring the relative importance of the HB, GB, and BP, respectively, and $w_1 + w_2 + w_3 = 1$. In addition, $rand1$, $rand2$, and $rand3$ are random numbers that are uniformly distributed in the range [0, 1].

The parameter D is used to evaluate the effect of damping level on vibration, as shown in the following:

$$D = \left(\frac{iter}{iter_{\max}}\right)^{-\alpha}, \quad (40)$$

where $iter$ is the current iteration number, $iter_{\max}$ the total number of iterations for optimization process, and α a constant parameter.

The parameter A is defined as:

$$A = [w_1.(HB^j - x_i^j)] + [w_2.(GP^j - x_i^j)] + [w_3.(BP^j - x_i^j)]. \quad (41)$$

The parameter is defined as p within the range of (0,1) to accelerate the convergence of the VPS algorithm. For each particle, P is compared with $rand$ if $P < rand$; then, $w_3 = 0$ and $w_2 = 1 - w_1$;

Step 4: The particles move in the search space to find a better result and may violate the side boundary. In order to handle this constraint, a harmony search-based approach is used in this algorithm;

Step 5: Steps 2 to 4 is repeated until the termination criterion is completed.

3.4. Enhanced Vibrating Particles System (EVPS)

In order to improve the results of the VPS algorithm through these techniques, the EVPS algorithm was developed so that the convergence speed increased and local optimum was prevented [36]. In this algorithm, the memory parameter acts as HB with the difference that it saves *Memory size* number of the best historically positions in the entire population. In case the best answer in each iteration is better than the worst value of memory, it is replaced by the worst value in memory. OHB (one of the best historically positions in entire population) is one row of memory that is randomly selected. Eqs. (39) and (41) of the VPS algorithms are replaced by Eqs. (42) and (43) of the EVPS algorithm, where (± 1) are used randomly:

$$[D.A.rand1 + OHB^j],$$

$$x_i^j = [D.A.rand2 + GP^j], \quad (42)$$

$$[D.A.rand3 + BP^j],$$

$$(\pm 1)(OHB^j - x_i^j),$$

$$A = (\pm 1)(GP^j - x_i^j), \quad (43)$$

$$(\pm 1)(BP^j - x_i^j),$$

$$w_1 + w_2 + w_3 = 1. \quad (44)$$

3.5. Particle Swarm Optimization (PSO)

PSO is one of the well-known algorithms, and it is widely used in many studies. This algorithm is inspired by swarm intelligence [37]. The positions and velocity of the particles are updated using the following equations to find the global optimum:

$$V_i[t+1] = WV_i[t] + r_1c_1(P_i[t] - X_i[t]) + r_2c_2(P_g[t] - X_i[t]), \quad (45)$$

$$X_i[t+1] = X_i[t] + V_i[t+1]. \quad (46)$$

In these equations, V and X express the velocity and position of each particle, respectively. In addition, P_i is the best position for the ith particles, P_g the global best position among all particles, and W is Inertia Weight. Further, c_1 and c_2 are the personal learning coefficient and global learning coefficient, respectively. Moreover, r_1 and r_2 are two random numbers that are uniformly distributed within (0, 1).

4. Numerical examples

A four-story RC frame with prismatic beams and, again, a frame with non-prismatic beams were taken into account to investigate the objectives of this study. The performance-based optimal seismic design of frames was performed at three performance levels IO, LS, and CP according to FEMA. The objective functions minimize the construction cost and CO_2 emissions. The live and dead loads were measured as 24 kN/m and 36 kN/m, respectively. There are some special approaches to increasing the convergence speed of algorithms [38,39] is used. In order to obtain the best results for this study, a strategy that was introduced by Kazemzadeh Azad [38] is used. In this strategy, to accelerate the convergence speed of the algorithms, the initial population with feasible solutions is replaced by a random population. In this study, the frames were optimized multiple times, and the candidate solution with the lowest penalty was placed as a candidate in the initial population and then, the optimization was performed.

4.1. RC frame with prismatic beams

This example is a four-story and two-span frame with prismatic beams. The height of each story is three meters, and the length of each span is 10 meters. The geometry, lateral loading, and grouping of members are shown in Figure 7, including eight column groups and four groups of beams. The procedure described for PBSD was also used to minimize the cost and carbon dioxide emissions at three performance levels, the results of which are presented below.

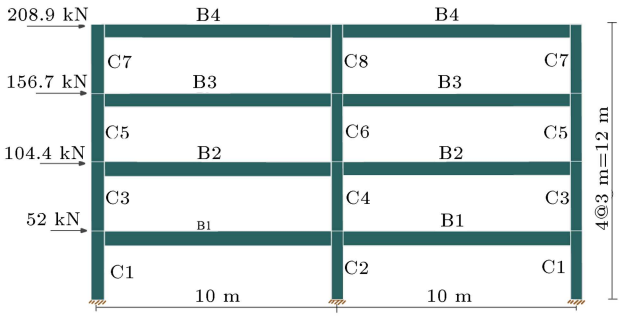

Figure 7. Geometry and grouping of the elements for frame with prismatic beams.

Table 5. Suitable parameters used for each of the algorithms.

CBO		Pop. size				
	Cost object	26				
	CO_2 object	22				
ECBO		Pop. size	CM size	Pro		
	Cost object	16	Pop. size/2	0.45		
	CO_2 object	16	Pop. size/2	0.45		
VPS		Pop. size	α	W1	W2	p
	Cost object	18	0.05	0.3	0.4	0.2
	CO_2 object	10	0.05	0.2	0.2	0.2
EVPS		Pop. size	α	W1	W2	p
	Cost object	18	0.05	0.2	0.6	0.2
	CO_2 object	18	0.05	0.2	0.2	0.2
PSO		Pop. size	Inertia weight	C1	C2	
	Cost object	26	2	2	2	
	CO_2 object	32	2	2	2	

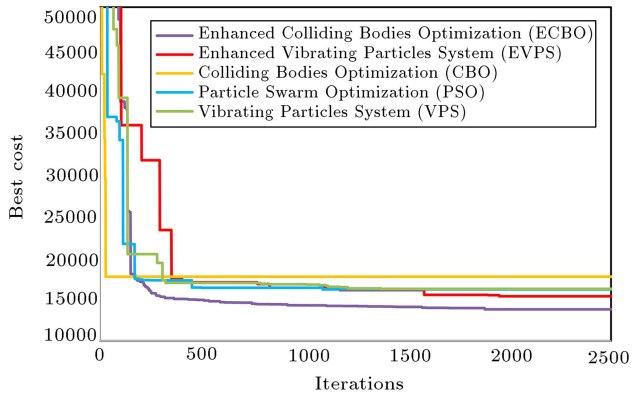

Figure 8. Comparison of the convergence curves of the algorithms for frame with prismatic beams to the lowest cost.

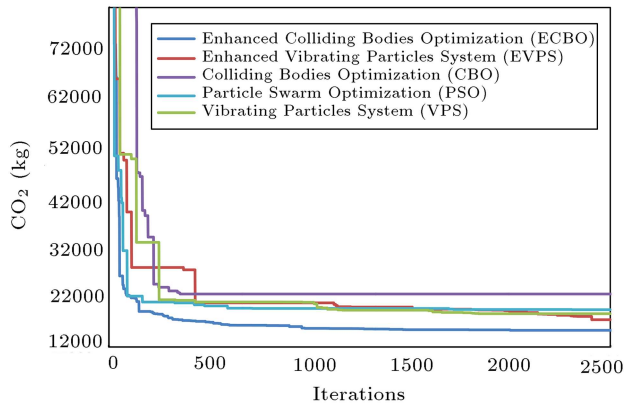

Figure 9. Comparison of the convergence curves of the algorithms for frame with prismatic beams to the lowest CO_2 emissions.

At the IO level of performance, five metaheuristic algorithms were used for optimization. The appropriate parameters used for each of the algorithms are listed in Table 5. The convergence curves of the algorithms for the lowest cost and lowest CO_2 emissions are compared in Figures 8 and 9, respectively. Table 6 presents the optimal results for all five algorithms. A comparison of the results shows that the ECBO algorithm outperforms the other algorithms in both objective functions; therefore, this algorithm was employed to solve the rest of the problem.

The results of the ECBO algorithm indicate that in the solution with the objective of minimizing cost, the best reported solution is 13770 euro with 15629 kg of carbon dioxide emissions (Table 7). In the solution with the objective of minimizing CO_2 emissions, the best reported solution is 15348 kg with 14082 euro of cost (Table 8). A percentage comparison of results indicates that in the solution based on the objective function of minimizing carbon dioxide emissions, with a 2.2% increase in cost, the CO_2 emissions would be reduced by 1.8%.

The distribution of the inter-story drift ratios obtained from pushover analysis for optimal designs at IO, LS, and CP performance levels with the objectives of minimizing the cost and CO_2 emissions is shown in Figures 10 and 11. Here, the vertical dash line indicates the permissible drift. The drift of stories should not exceed the specified limits.

Figure 12 shows the relationship between the optimal cost and optimal CO_2 emissions in the performance-based optimal seismic design at three performance levels, where the objective functions are either CO_2 emissions or economic cost. These relationships indicate that in RC frames with prismatic beams, compared to a cost-optimization design, a design based on minimizing CO_2 emissions can reduce the CO_2 emissions. At the LS and CP performance levels, the optimal design of frames with the objective of minimizing CO_2 has more effect on reducing CO_2 emissions.

4.2. The frame with non-prismatic beams

In this example, the frame of the first example was extended, where the beams are non-prismatic. The lateral loading as well as grouping of beams and columns are shown in Figure 13. Performance-based optimal seismic design was used for this frame to minimize objective functions at three performance levels.

According to the results of the ECBO algorithm at the IO performance level, in the solution with the objective of minimizing the costs, the best reported solution is 12752.19 euro with 15004 kg of carbon dioxide emissions (Table 9). In the solution with the objective of minimizing CO_2 emissions, the best reported solution is 14368 kg at a cost of 12759 euro (Table 10). A percentage comparison of results reveals that in the solution based on the objective function

Table 6. Comparative results of the algorithms for frame with the prismatic beams at Immediate Occupancy (IO) level.

		EVPS	ECBO	VPS	CBO	PSO
Cost objective	Best cost (€)	15340	13770	16226	17692	16160
	SD	1717	307	2780.66	551.3	2577
	Average (€)	16278.6	14143.7	17821.6	18815	17627.6
CO_2 objective	Best CO_2 (kg)	17745	15348	18674	22621	19483
	SD	866.2	635.9	1750.7	901.3	1144
	Average (kg)	18830.11	16212.2	20953.4	23940.88	20981

Table 7. Optimal results of the cost objective for frame with the prismatic beams at Immediate Occupancy (IO) level.

		Cost objective			
		b (mm)	h (mm)	A_s top	A_s bottom
Beam group no.	1	350	750	3#11	3#8
	2	350	1050	4#9	4#6
	3	350	900	3#10	2#8
	4	350	950	4#8	4#6
Column group no.	1	350	850	8#8	
	2	350	800	6#8	
	3	350	800	10#6	
	4	300	750	8#6	
	5	300	750	8#6	
	6	300	700	6#8	
	7	300	700	12#7	
	8	250	300	4#6	
Average		14143.7 €			
Std deviation		307			
Best solution		Cost 13770 €(with 15629 kg of CO_2 emissions)			

Table 8. Optimal results of CO_2 emissions objective for frame with the prismatic beams at Immediate Occupancy (IO) level.

		CO_2 objective			
		b (mm)	h (mm)	A_s top	A_s bottom
Beam group no.	1	350	950	3#10	5#5
	2	350	1050	5#8	3#7
	3	350	1050	3#10	4#6
	4	350	1000	3#9	4#6
Column group no.	1	350	800	8#7	
	2	350	750	10#6	
	3	350	800	6#8	
	4	300	650	10#5	
	5	300	700	8#6	
	6	300	650	12#6	
	7	300	700	12#7	
	8	250	250	12#3	
Average		16212.2 kg			
Std deviation		635.9			
Best solution		CO_2 15347.8 kg (at a cost of 14082 €)			

of minimizing carbon dioxide emissions, with a 0.054% increase in the cost, CO_2 emissions would be reduced by 4.2%.

Figures 14 and 15 show the distribution of the inter-story drift ratios for the frame with non-prismatic beams at IO, LS, and CP performance levels with the objectives of minimizing the cost and CO_2 emissions, respectively.

Figure 16 shows the relationship between the optimal cost and optimal CO_2 emissions in the

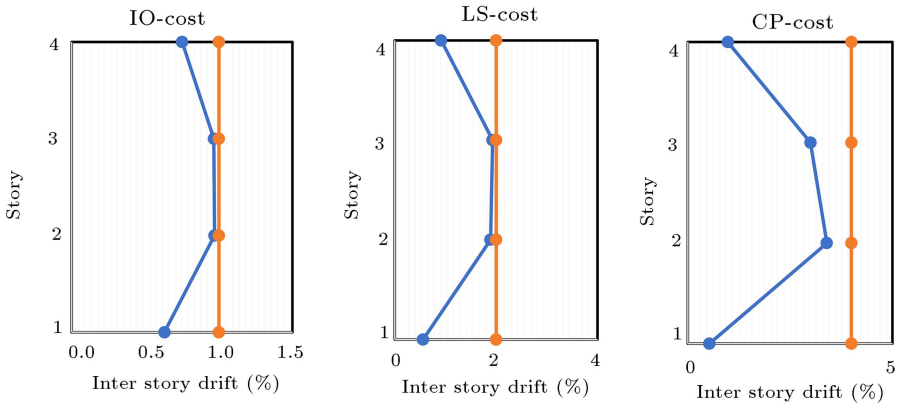

Figure 10. Inter-story drift ratio for the frame with prismatic beams at the three performance levels in the cost objective.

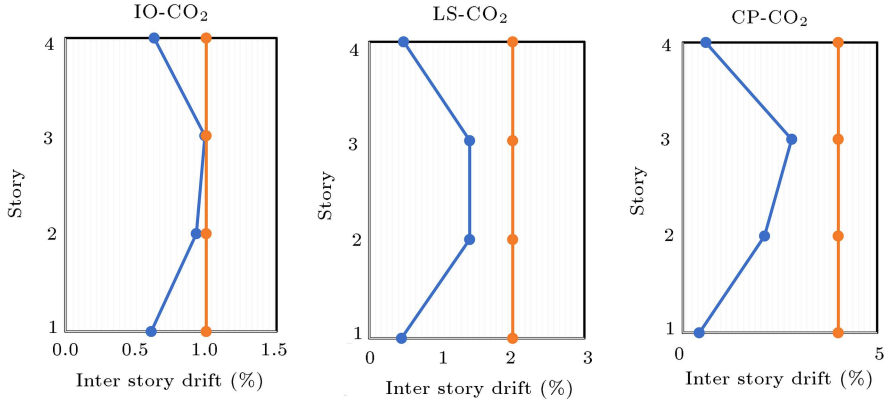

Figure 11. Inter-story drift ratio for the frame with prismatic beams at the three performance levels in the CO_2 objective.

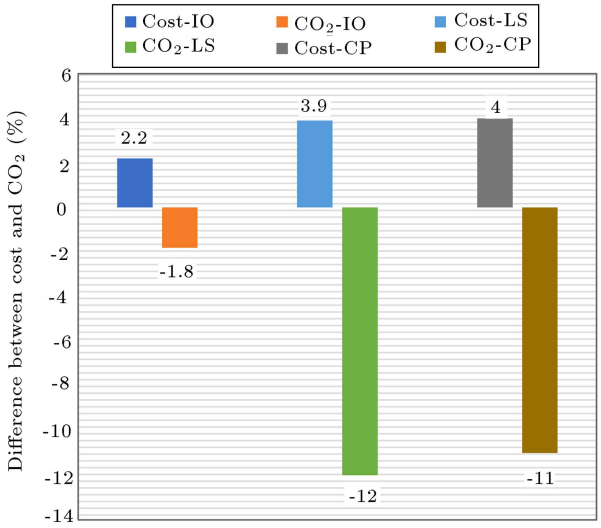

Figure 12. The relationship between optimal cost and optimal CO_2 emissions for the frame with prismatic beams.

performance-based optimal seismic design of the frame with non-prismatic beams. At the IO and LS performance levels, the increase in optimal cost is smaller. Therefore, at these levels, design with the objective

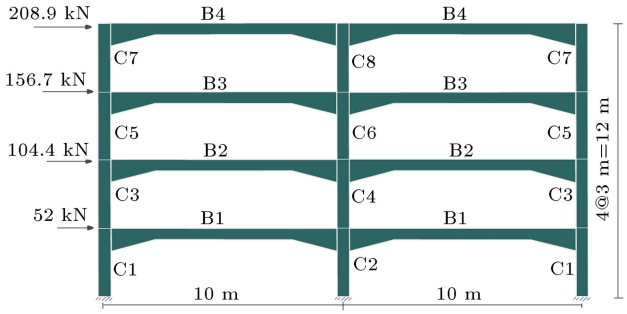

Figure 13. Geometry and grouping of the elements for the frame with non-prismatic beams.

of minimizing CO_2 emissions in addition to reduction CO_2 have optimal cost.

5. Concluding remarks

In this paper, nonlinear static pushover analysis was incorporated to the structural optimization strategy for performance-based optimal seismic design of Reinforced Concrete (RC) frames with prismatic beams and frames with non-prismatic beams. The constraints were controlled in two steps: first, the equivalent static analysis was performed and strength-based constraint

Table 9. Optimal results of cost objective for frame with the non-prismatic beams at Immediate Occupancy (IO) level.

		b (mm)	h_1 (mm)	h_2 (mm)	A_{s1} top	A_{s1} bottom	A_{s2} top	A_{s2} bottom	TLR%
Beam group no.	1	350	700	450	4#10	3#6	5#8	5#7	10
	2	350	950	700	5#8	4#8	2#8	4#6	20
	3	350	950	750	5#8	4#8	3#6	2#8	20
	4	350	800	800	4#10	2#9	4#6	5#6	10
Column group no.	1	400	1000				6#10		
	2	450	1100				10#8		
	3	350	850				6#8		
	4	400	1000				8#8		
	5	350	750				10#6		
	6	350	800				10#6		
	7	300	700				12#7		
	8	250	500				8#6		
Average		14058 €							
Std deviation		1731.8							
Best solution		Cost 12752.19 € (with 15004 kg of CO_2 emissions)							

Table 10. Optimal results of CO_2 objective for frame with the non-prismatic beams at Immediate Occupancy (IO) level.

		b (mm)	h_1 (mm)	h_2 (mm)	A_{s1} top	A_{s1} bottom	A_{s2} top	A_{s2} bottom	TLR%
Beam group no.	1	350	800	750	4#9	2#9	4#7	4#6	10
	2	350	950	800	4#10	4#6	5#6	4#6	15
	3	350	1000	650	5#8	2#10	4#6	4#6	20
	4	350	850	800	5#8	2#10	5#6	4#6	10
Column group no.	1	450	1050				6#10		
	2	400	850				12#6		
	3	350	800				10#6		
	4	350	800				10#6		
	5	300	750				10#6		
	6	350	800				10#6		
	7	300	700				8#9		
	8	250	600				6#7		
Average		15030 kg							
Std deviation		801.77							
Best solution		CO_2 14368 kg (at a cost of 12759 €)							

were controlled; then, the nonlinear pushover analysis was carried out at three performance levels according to the FEMA code and the maximum inter-story drift was investigated. In order to identify the most competent algorithm for solving the problem, five metaheuristic algorithms including Particle Swarm Optimization (PSO), Colliding Bodies Optimization (CBO), Enhanced Colliding Bodies Optimization (ECBO), Vibrating Particles System (VPS), and Enhanced Vibrating Particles System (EVPS) were used to op-

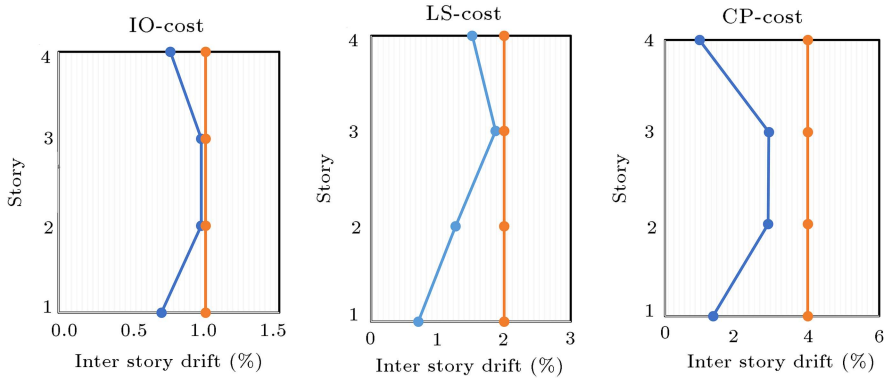

Figure 14. Inter-story drift ratio for the frame with non-prismatic beams at the three performance levels in the cost objective.

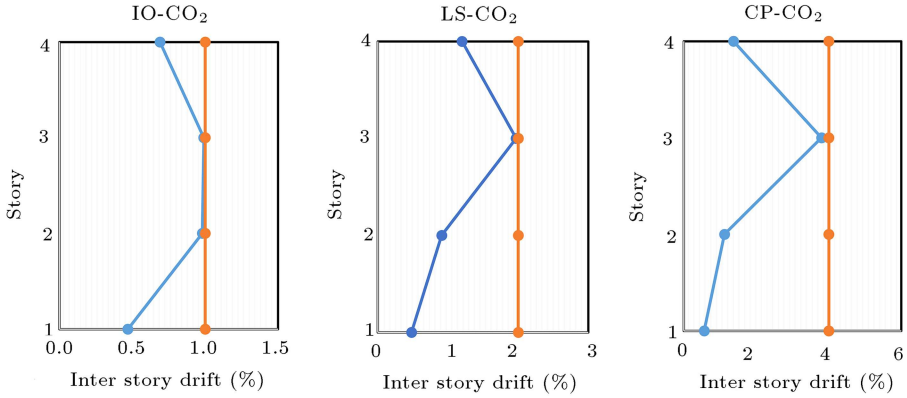

Figure 15. Inter-story drift ratio for the frame with non-prismatic beams at the three performance levels in the CO_2 objective.

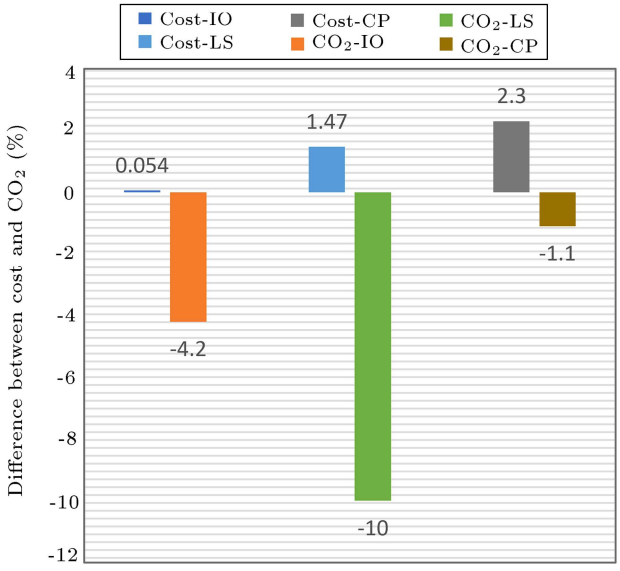

Figure 16. The relationship between optimal cost and optimal CO2 emissions for frame with non-prismatic beams.

timize the objectives at the Immediate Occupancy (IO) performance level, and the rest of the problems were solved using the selected competent algorithm. Comparison of the performance of the algorithms in the first example demonstrated that ECBO performed better than the other algorithms. The relationships between optimal cost and optimal CO_2 emissions in Performance Based Optimal Seismic Design (PBOSD) for three performance levels showed that in the design of RC frames with the objective of minimizing CO_2 emissions, CO_2 could be reduced compared to the design with the objective of optimizing cost. In frames with prismatic beams at performance levels, with 2.2% to 4% increase in cost, CO_2 was reduced by 1.8% to 12%, and for frames with non-prismatic beams with 0.05% to 2.3% increase in cost, the reduced CO_2 was 1.1% to 10%.

References

1. FEMA-273, "NEHRP guideline for the seismic rehabilitation of buildings", Federal Emergency Management Agency (1997).
2. Zou, X.K. and Chan, C.M. "Optimal seismic performance-based design of reinforced concrete buildings using nonlinear pushover analysis", *Eng. Struct.*, **27**(8), pp. 1289–1302 (2005). https://doi.org/10.1016/j.engstruct.2005.04.001
3. Zou, X.K. and Chan, C.M. "An optimal resizing technique for seismic drift design of concrete build-

ings subjected to response spectrum and time history loadings", *Comput. Struct.*, **83**, pp. 1689–1704 (2005). https://doi.org/10.1016/j.compstruc.2004.10.002

4. Zhang, C. and Tian, Y. "Simplified performance-based optimal seismic design of reinforced concrete frame buildings", *Eng. Struct.*, **185**, pp. 15–25 (2019). https://doi.org/10.1016/j.engstruct.2019.01.108
5. Papavasileiou, G.S. and Charmpis, D.C. "Seismic design optimization of multi-storey steel-concrete composite buildings", *Comput. Struct.*, **170**, pp. 49–61 (2016). https://doi.org/10.1016/j.compstruc.2016.03.010
6. Gholizadeh, S. "Performance-based optimum seismic design of steel structures by a modified firefly algorithm and a new neural network", *Adv. Eng. Softw.*, **81**, pp. 50–65 (2015). https://doi.org/10.1016/j.advengsoft.2014.11.003
7. Kaveh, A., Farahmand Azar, B., Hadidi, A., Rezazadeh Sorochi, F., and Talatahari, S. "Performance-based seismic design of steel frames using ant colony optimization", *J. Constr. Steel Res.*, **66**, pp. 566–574 (2010). https://doi.org/10.1016/j.jcsr.2009.11.006
8. Zou, X.K., Chan, C.M., Li, G., and Wang, Q. "Multiobjective optimization for performance-based design of reinforced concrete frames", *J. Struct. Eng.*, **133**(10), pp. 1462–1474 (2007). DOI: 10.1061/(ASCE0)733-9445(2007)133:10(1462)
9. Mitropoulou, C.C., Lagaros, N.D., and Papadrakakis, M. "Life-cycle cost assessment of optimally designed reinforced concrete buildings under seismic actions", *Reliab. Eng. Syst. Saf.*, **96**(10), pp. 1311–1331 (2011). https://doi.org/10.1016/j.ress.2011.04.002
10. Lagaros, N.D. and Magoula E. "Life-cycle cost assessment of mid-rise and high-rise steel and steel-reinforced concrete composite minimum cost building designs", *Struct. Des. Tall Spec. Build*, **22**(12), pp. 954–974 (2011). https://doi.org/10.1002/tal.752
11. Kaveh, A., Laknejadi, K., and Alinejad, B. "Performance-based multi-objective optimization of large steel structures", *Acta Mech.*, **223**(2), pp. 355–369 (2012). https://doi.org/10.1007/s00707-011-0564-1
12. Park, H.S., Hwang, J.W., and Oh, B.K. "Integrated analysis model for assessing CO_2 emissions, seismic performance, and costs of buildings through performance-based optimal seismic design with sustainability", *Energy Build.*, **158**, pp. 761–775 (2018). https://doi.org/10.1016/j.enbuild.2017.10.070
13. Pachauri, R.K. and Reisinger, A. "United Nations Intergovernmental Panel on Climate Change. Climate change 2007: synthesis report. Contribution of working groups I, II and III to the fourth assessment report of the intergovernmental panel on climate change", Geneva, Switzerland (2007).
14. Camp, C.V. and Huq, F. "CO_2 and cost optimization of reinforced concrete frames using a big bang-big crunch algorithm", *Eng. Struct. J.*, **48**(2), pp. 363–372 (2013). https://doi.org/10.1016/j.engstruct.2012.09.004
15. Camp, C.V. and Assadollahi, A. "CO_2 and cost optimization of reinforced concrete footings subjected to uniaxial uplift", *J. Build. Eng.*, **3**, pp. 171–183 (2015). https://doi.org/10.1016/j.jobe.2015.07.008
16. Yepes, V., Gonzalez-vidosa, F., Alcala, J., and Villalba, P. "CO_2-optimization design of reinforced concrete retaining walls based on a VNS-threshold acceptance strategy", *J. Comput. Civ. Eng.*, **26**(3), pp. 378–386 (2012). http://dx.doi.org/10.1061/(ASCE)CP.1943-5487.0000140
17. Kaveh, A., Izadifard, R.A., and Mottaghi, L. "Optimal design of planar RC frames considering CO_2 emissions using ECBO, EVPS, and PSO metaheuristic algorithms", *J. Build. Eng.*, **28**, p. 101014 (2020). https://doi.org/10.1016/j.jobe.2019.101014
18. Mergos, P.E. "Seismic design of reinforced concrete frames for minimum embodied CO_2 emissions", *Energy Build.*, **162**, pp. 177–186 (2018). https://doi.org/10.1016/j.enbuild.2017.12.039
19. Yeo, D. and Potra, F.A. "Sustainable design of reinforced concrete structures through CO_2 emission optimization", *J. Struct. Eng*, **141**(3), B4014002 (2015). https://doi.org/10.1061/(ASCE)ST.1943-541X.0000888
20. Oh, B.K., Park, J.S., Choi, S.W., and Park, H.S. "Design model for analysis of relationships among CO_2 emissions, cost, and structural parameters in green building construction with composite columns", *Energy Build.*, **118**, pp. 301–315 (2016). https://doi.org/10.1016/j.enbuild.2016.03.015
21. McKinstray, R., Lim, J.B.P., Tanyimboh, T.T., Phan, D.T., and Sha, W. "Comparison of optimal designs of steel portal frames including topological asymmetry considering rolled, fabricated and tapered sections", *Eng. Struct.*, **111**, pp. 505–524 (2016). https://dx.doi.org/10.1016/j.engstruct.2015.12.028
22. Kaveh, A., Kabir, M.Z., and Bohlool, M. "Optimum design of three-dimensional steel frames with prismatic and non-prismatic elements", *Eng. Comput.*, **36**, pp. 1011–1027 (2019). https://doi.org/10.1007/s00366-019-00746-9
23. Solat Yavari, M., Du, G., Pacoste, C., and Karoumi, R. "Environmental impact optimization of reinforced concrete slab frame bridges", *J. Civ. Eng. Archit.*, **11**(4), pp. 313–324 (2017). DOI: 10.17265/1934-7359/2017.04.001
24. Kaveh, A., Mottaghi, L., and Izadifard, R.A. "Sustainable design of reinforced concrete frames with non-prismatic beams", *Eng. Comput.*, 123456789 (2020). https://doi.org/10.1007/s00366-020-01045-4

25. A.C. Institute, Building code requirements for structural concrete and commentary, ACI 318-08 (2008).

26. FEMA-356, *Prestandard and Commentary for the Seismic Rehabilitation of Buildings*, Federal Emergency Management Agency (2000).

27. Fathali, M.A. and Hoseini Vaez, S.R. "Optimum performance-based design of eccentrically braced frames", *Eng. Struct.*, **202** (2020). https://doi.org/10.1016/j.engstruct.2019.109857

28. Moehle, J.P. and Mahin, S.A., *Observations on the Behavior of Reinforced Concrete Buildings During Earthquakes*, American Concrete Institute, SP-127 (1991).

29. PEERS and OpenSEES, *Open System for Earthquake Engineering Simulation*, Pacific Earthquake Engineering Research Centre, University of California, Berkeley (2012).

30. The Language of Technical Computing, MATLAB. Math Works Inc (2016).

31. Kaveh, A. and Mahdavi, V.R. "Colliding bodies optimization: A novel meta-heuristic method", *Comput. Struct.*, **139**, pp. 18–27 (2014). https://doi.org/10.1016/j.compstruc.2014.04.005

32. Kaveh, A. and Ilchi Ghazaan, M. "Enhanced colliding bodies optimization for design problems with continuous and discrete variables", *Adv. Eng. Softw.*, **77**, pp. 66–75 (2014). https://doi.org/10.1016/j.advengsoft.2014.08.003

33. Kaveh, A. and Ghafari, M.H. "Optimum design of castellated beams: Effects of composite action and semi-rigid connections", *Sci. Iran.*, **25**(1), pp. 162–173 (2018). https://doi.org/10.24200/sci.2017.4195

34. Kaveh, A. and Sabeti, S. "Optimal design of monopile offshore wind turbine structures using CBO, ECBO, and VPS algorithms", *Sci. Iran.*, **26**(3A), pp. 1232–1248 (2019). https://doi.org/10.24200/sci.2018.20090

35. Kaveh, A. and Ilchi Ghazaan, M. "A new metaheuristic algorithm: vibrating particles system", *Sci. Iran.*, **24**(2), pp. 1–32 (2017). https://doi.org/10.24200/sci.2017.2417

36. Kaveh, A., Hoseini Vaez, S.R., and Hosseini, P. "Enhanced vibrating particles system algorithm for damage identification of truss structures", *Sci. Iran.*, **26**(1A), pp. 246–256 (2019). https://doi.org/10.24200/sci.2017.4265

37. Eberhart, R. and Kennedy, J. "A new optimizer using particle swarm theory", *Proc. Sixth Int. Symp. micro Mach. Hum. Sci.*, pp. 1942–1948 (1995). https://doi.org/10.1109/MHS.1995.494215

38. Kazemzadeh Azad, S. "Seeding the initial population with feasible solutions in metaheuristic optimization of steel trusses", *Eng. Optim.*, **50**(1), pp. 1–17, no. February (2017). http://dx.doi.org/10.1080/0305215X.2017.1284833

39. Kazemzadeh Azad, S., Hasançebi, O., and Kazemzadeh Azad, S. " Upper bound strategy for metaheuristic based design optimization of steel frames", *Adv. Eng. Softw.*, **57**, pp. 19–32 (2013). https://doi.org/10.1016/j.advengsoft.2012.11.016

Biographies

Ali Kaveh was born in 1948 in Tabriz, Iran. After graduation from the Department of Civil Engineering in the University of Tabriz in 1969, he continued his studies on Structures at Imperial College of Science and Technology in London University and received his MSc, DIC, and PhD degrees in 1970 and 1974. He then joined the Iran University of Science and Technology. Professor Kaveh is the author of 700 papers published in international journals and has presented 150 papers at national and international conferences. He has authored 23 books in Persian and 10 books in English published by Wiley, Research Studies Press, American Mechanical Society, and Springer.

Lida Mottaghi was born in 1987 in Marand. She obtained her MS degree in Earthquake Engineering from the Khajeh Nasir Toosi University (KNTU), Iran. At present, she is a PhD student at Imam Khomeini International University (IKIU), Gazvin, Iran. She works on the optimum design of RC frames via the metaheuristic methods.

Ramezan Ali Izadifard was born in 1966 in Frydonkenar, in the north of Iran. He studied structural engineering at Isfahan University of Technology and Shiraz University and received his BS, MSc, and PhD degrees in 1989, 1992, and 2008, respectively. He is the author of more than 50 papers published in international journals or presented papers at professional conferences. He is currently teaching and researching at Imam Khomeini International University.